Magdalena Ridge Observatory interferometer: UT#1 site installation, alignment and test

Christian Bastin[a]*, Olivier Pirnay[a], Vincent Moreau[a], Carlo Flebus[a], Andres Olivares[b]

[a]Advanced Mechanical and Optical Systems (AMOS s.a.),
LIEGE science park, B-4031 Angleur, BELGIUM;
[b]New Mexico Institute of Mining and Technology, Socorro, New Mexico, USA

ABSTRACT

The deployment of the Magdalena Ridge Observatory Interferometer has resumed in 2016. AMOS, in charge of the development of the unit telescopes, has completed the installation of the first telescope on the Ridge. The compactness of the system allows for a fast installation, as only the optics and their supports need to be transported in separate crates. The installation has been followed by the alignment procedure combining metrological and optical measurement techniques and aiming at optimizing the pupil stability and image quality. Finally, the performance of the telescope has been evaluated on the sky as part of the site acceptance.
Keywords: telescope, interferometry, optical array, testing, site, elevation over elevation, elevation over elevation

1. INTRODUCTION

The Magdalena Ridge Observatory Interferometer (MROI) is a high-sensitivity imaging optical/IR interferometer in construction on the Magdalena Ridge. It is situated at the altitude at 3230 m, 45 km West of Socorro, NM.

Up to 10 unit telescopes will be operated simultaneously to produce model-independent images. These telescopes can be relocated on 28 different piers spread on a "Y" shape array. With baselines from 7.8 m to 347 m, the instrument will generate sub-milliarcsecond angular resolution sharp images in the range of 0.6 to 2.4 µm wavelength.

The instrument optical throughput is optimized in order to image faint objects: one key piece is the 1.4 m unit telescope in which the stellar light is collected with only three mirrors possible due to the afocal elevation over elevation configuration.

The major science goals are the study of the earliest phases of star and planet formation, the complex astrophysical processes in single and multiple star systems, and the environments of black holes in the hearts of other galaxies.

The design of all major systems for the interferometer has been completed. AMOS has concluded the manufacturing and testing of the first unit telescope in factory in Belgium. It has been dismounted and shipped to New Mexico, where it was stored in a safe place, waiting to be installed on site. The site was ready in 2016, and the installation of the first telescope in the observatory was resumed. This installation is presented in this paper.

In parallel, the structure and bearing of the second and third telescopes are already assembled. Construction of the Beam Combining Facility (BCF) which includes the interferometric laboratory, the delay line area, control room and administrative space, has been completed. The manufacturing of the first enclosure is almost completed, assembly and on-site testing to be performed on July-2018.

*christian.bastin@amos.be; phone 32 4 361 40 40; www. amos.be

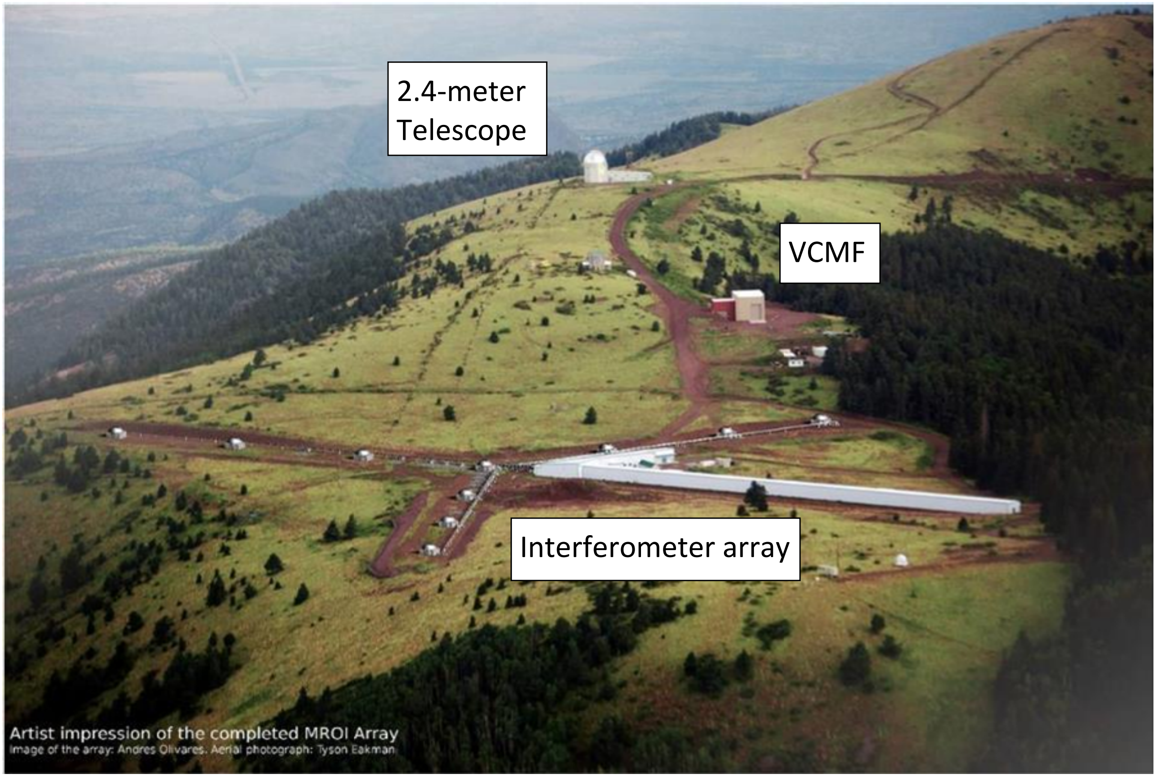

Figure 1: Artistic view of the MRO Interferometer in extended configuration. The buildings construction was completed in 2007. (Courtesy of MRO)

2. TELESCOPE DESIGN OVERVIEW

2.1 Requirement specifications

The telescope is a Mersenne beam compressor supported by an elevation-over-elevation mount. The system consists of a 1425 mm diameter f/2.25 concave parabolic primary combined with a 115 mm diameter convex parabolic secondary. The M1-M2 spacing is 2936.25 mm. The 95 mm diameter collimated beam is sent out of the telescope through the outer elevation axis due to a flat mirror (M3) rotating around the inner elevation axis. The tracking speed of the M3 is half of the speed of the inner elevation axis. The angular range (field of regard) is -50/+40 degrees and ±60 degrees from zenith for the inner elevation axis and the outer elevation axis respectively.

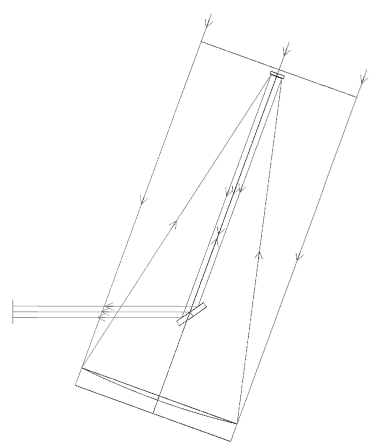

Figure 2. Optical configuration of the MROI unit telescope.

The ambitious objectives of the MRO Interferometer led the system architects to specify stringent requirements for the unit telescope. The performance summarized here below will be maintained in severe environmental conditions.

- Overall image quality: 63 nm RMS
- Optical obscuration less than 5%
- Pupil stability: 0.5 mm over the entire field of regard
- Pointing error less than 20 arcsec over the full night
- Open loop tracking better than 1 arcsec
- Closed loop tracking: 0.02 arcsec and 0.03 arcsec RMS respectively for the mount and the wind shake residual error. A 200 Hz bandwidth fast steering actuator is implemented at the level of the secondary mirror for tip-tilt correction.
- Optical Path Length (OPL) Stability: 23 nm RMS for a 12 ms exposure time frame

2.2 Mount design

The two axes of the elevation-over-elevation mount are connected to each other by means of a gimbal structure. The fork is the fixed part of the telescope. It supports the outer elevation axis of the gimbal and provides a stiff and stable interface with the pier. The fork also provides the interface for the Nasmyth table where the closed loop sensors are installed by the final user. The gimbal is a closed frame box structure. It locates the two main axes concurring and perpendicular to each other. The gimbal supports the telescope tube through the inner elevation axis. The tube supports and maintains stability of the M1, M2 and M3 units in the entire operational range.

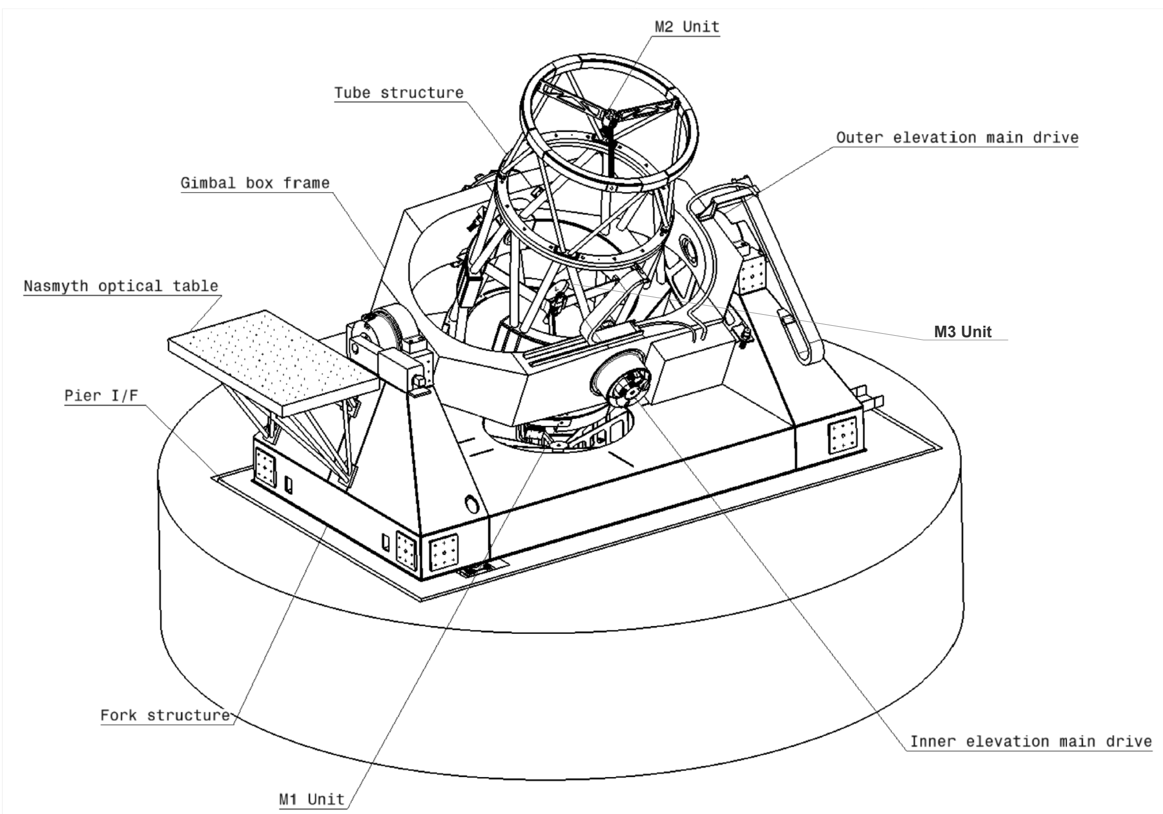

Figure 3. MROI unit telescope, overall view.

Total weight: 15 500 kg – Overall dimensions (L x W x H): 6160 x 2920 x 4350 mm.

The throughput of the telescope is greatly enhanced by the fact that only three reflections occur from the primary mirror to the output collimated beam. As a drawback, the elevation-over-elevation mount necessitates a large free opening in the tube to avoid any obscuring of the output beam.

The interface with the pier is designed as a kinematic support in order to avoid inducing stress and deformation to the telescope structure in case of misalignment or instability of the pier interface. It also allows accurate re-positioning of the telescope after relocation on another pier of the array.

As the inertia and wind exposure are the same order of magnitude for both axes, the components of each axis are identical except for the bearings. The servo controller is a UMAC Delta Tau dedicated to the main axes. Two liquid cooled DC brushless motors are implemented on each axis (one on each shaft). The UMAC is connected to the SERVOSTAR® motor drives through an analog current input. The absolute position feedback is given by a resolver and the high accuracy position feedback is provided by a circumferential-scale drum encoder with four scanning heads. The signal interpolation is performed by a dedicated card in the UMAC.

The unit telescope control system (UTCS) is developed with the LabView® programming language [3]. The kernel of the system makes use of the TCSpk from TPOINT™. Pointing directions and trajectories are downloaded to the axis servo-controllers as position set points related to absolute time. A graphical user interface is provided for engineering operation e.g. in stand-alone mode. In the normal operation mode, the UTCS is under the control of the interferometer control system (ICS) via a dedicated socket server.

2.3 Key features

The design of the telescope mount was driven by four constraints: the tracking performance, the optical pathlength stability, the pupil stability and the image quality. The first two are affected by the dynamic behavior of the system while the last two are influenced by static or quasi-static structural deformation only.

The tight specifications necessitated extensive optimizations and an accurate control of the error budgets. The dynamic performance could be met only by maximizing the natural frequencies of the structure and a proper optimization of the control system. Trade-off analyses and numerous iterative FEM optimizations were necessary in order to meet the image quality and pupil stability requirements. As a result, a compensation strategy based on the change in position of M2 as a function of the temperature and the pointing direction is implemented. This enables the telescope to maintain the image quality, the pupil stability and the pointing accuracy under control in the entire field of regard and temperature operational range.

The compensation law is at first elaborated by analysis and later adjusted with real measurements of the image quality by means of a retractable wavefront sensor that will be used as a calibrator.

A comprehensive presentation of the unit telescope design and the engineering approach are discussed in 2.

3. ASSEMBLY, INTEGRATION AND TEST IN FACTORY

The telescope mount was fully assembled, integrated and tested in factory at AMOS before being shipped to New Mexico. The main alignment activities performed in factory were

- Main axis alignment (see Figure 4)
- M3 mechanism alignment
- Main axis balancing and friction measurement
- System identification and main axis tuning
- Wavefront sensor alignment

Figure 4: Main axes measurement by means of the laser tracker

Following these activities, the factory acceptance tests took place, including following tests:

- M2 mechanism performance
- Telescope control system functionality
- Mount performance
- Optical path length stability
- Pupil stability

These activities are summarized in [4]. The performances and functionalities are verified by test not only because it is required by the customer but also on account that this is the only way to drastically reduce the risk of major difficulty during on-site installation and commissioning.

4. SITE INSTALLATION AND ALIGNMENT

Following successful factory acceptance, the telescope mount was packed for transport. Thanks to the compactness of the mount, the whole telescope fits inside a custom crate. This also allows to shorten the installation time needed on site.

Since the enclosure was not available when the site installation started, the telescope was installed in the visitors center and maintenance facility (VCMF) of the observatory, located next to the interferometer array (see Figure 1). Observations are possible from this building by opening the rolling door, but this allows only access to a reduced part of the sky.

The first operation on site was to unpack the telescope mount and to locate it on the maintenance station. This was done with the help of a crane truck as shown on Figure 5.

The next step was to integrate the optics in their cells. M1 cell is shown on Figure 6. The mirrors are then integrated in the mount, and preliminary aligned with a laser tracker.

In parallel, the mount is connected to the electrical cabinets and the good health of each mechanism is checked. The thermal control of the cabinets and motors is also restarted and tuned.

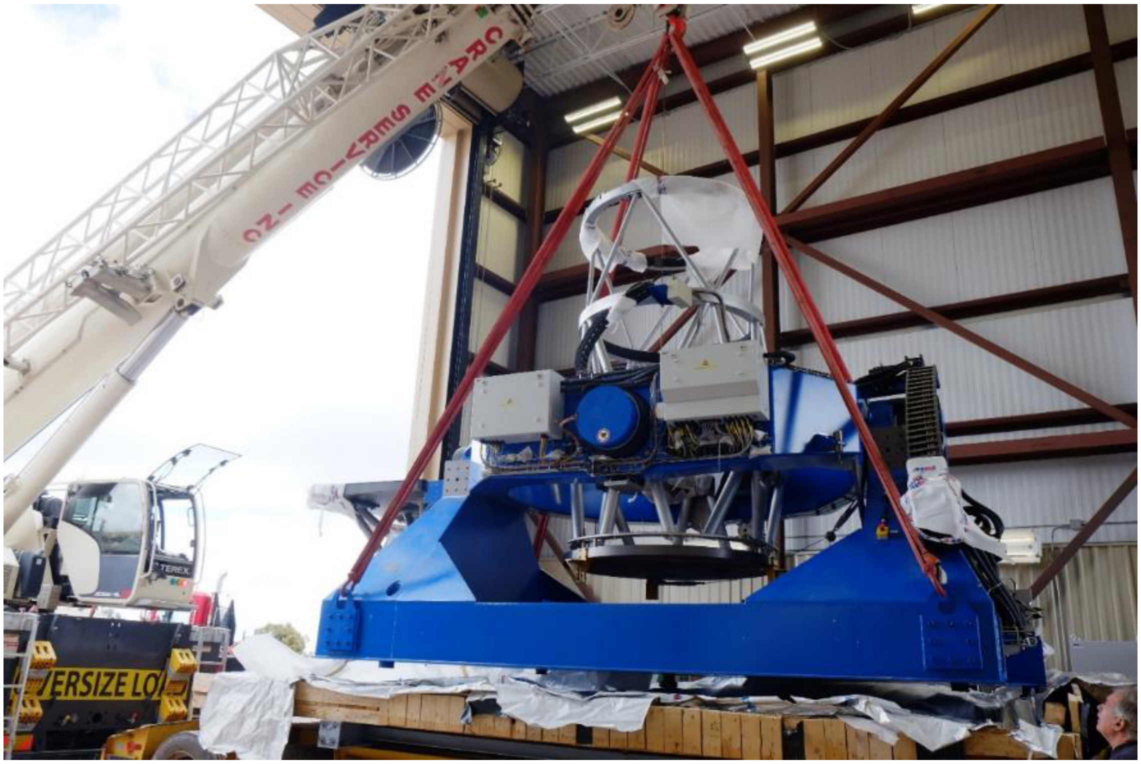

Figure 5. Installation of the telescope mount (without optics) in the VCMF

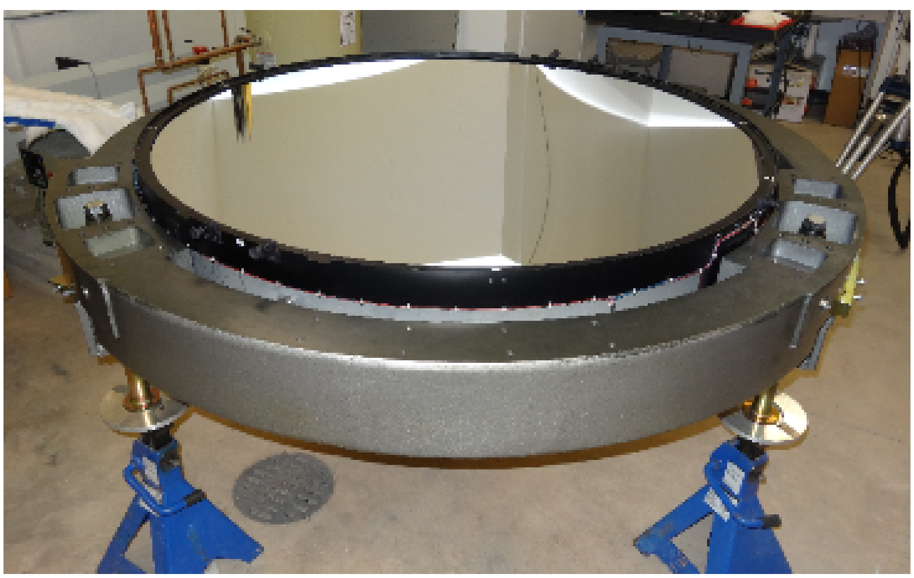

Figure 6. M1 installed in its cell

5. SITE TESTING

5.1 Mount performance

Once the telescope is fully integrated (mount and optics), the next step is to optimize and test the mount performance (which does not need access to the sky).

Each axis is first identified by injecting white noise in the system. The control loop is then tuned, with the goal to achieve a high control bandwidth, while keeping enough stability margins (at least 45 deg phase margin, and 10db gain margin). After tuning, the wind-free performances are measured on each axis, based on encoder signal. The result is shown on Figure 7 for the inner axis (without and with filtering by the Fast Tip Tilt Assembly).

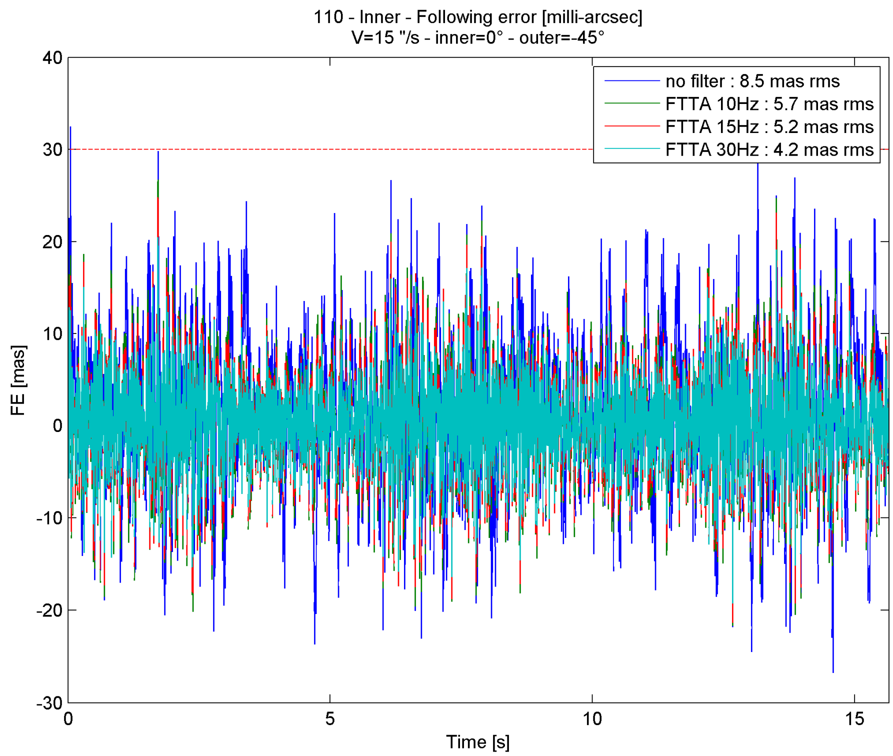

Figure 7. Mount error in wind free environment (units: milli-arcseconds – mas)

While the performances in wind-free environment are determined by measurement, the contribution of the wind disturbance can be evaluated only by analysis.

The Von Karman wind model is used for this analysis. It gives the one-sided power spectral density (PSD) of wind speed:

$$S_U(f) = (IU)^2 \cdot \frac{4L}{U} \cdot \frac{1}{(1+70.78\frac{L^2}{U^2}f^2)^{5/6}} \quad (1)^2$$

where:

S_U	is the power spectral density of the wind speed [(m/s)²/Hz]
I	is the turbulence intensity
U	is the mean speed of the wind outside the dome [m/s]
L	is the length scale of turbulence [m]
f	is the considered frequency [Hz]

In the present analysis, the mean speed is 10 m/s, the turbulence intensity is 0.12 and the length scale equals 5 m

Figure 8 shows for inner axis:

- Wind PSD of Von Karman model
- Transfer function of torque disturbance rejection
- Wind shake residual (tracking error of the axis due to wind disturbance) when the telescope operates with optical feedback. It is calculated as follow:

$$y_{rms} = \sqrt{\int_0^{\infty} PSD(f) \cdot \left[NR(f) \cdot \frac{s}{s + 2\pi f_{-3dB}}\right]^2 df} \tag{2}$$

where f_{-3dB} is 0.1 Hz for the guider and up to 30 Hz for the fast tip-tilt system.

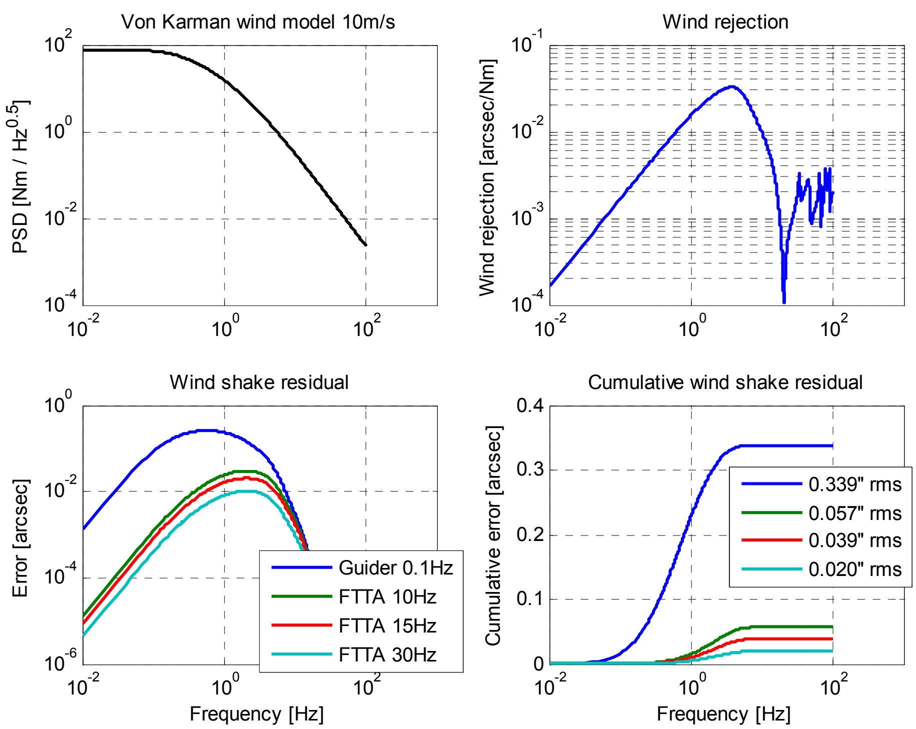

Figure 8. Wind shake residuals

The performance achieved on each axis (Inner, Outer and M3) is in line with the requirements

5.2 Pupil stability alignment and test

The pupil stability can also be tested directly without need of star light.

The output pupil position is defined as the position of the center of the image of the telescope primary mirror as seen through the combination of the secondary and tertiary mirrors (the projected telescope pupil image) from a location mechanically independent of the telescope.

The stability of each exit pupil during observation is critical as the fringes visibility depends on the overlapping surface of the combined UT pupils. Matching between UT exit pupils and beam combiner entrance pupil is also a critical aspect in order to prevent vignetting. It is required that the pupil position of each unit telescope varies by less than ±0.5mm over the operational field of regard.

In order to make possible the optical determination of the location of the center of the projected telescope pupil image, a ring of 4 light-emitting diodes (LEDs) is mounted on the M1 stop, oriented to illuminate the secondary mirror. Tracking of the LED images position allow to measure the pupil stability. The measure is made by imaging the pupil on a CMOS sensor that is mounted onto the Nasmyth table (see Figure 9).

The initial (mechanical) alignment made previously allows to have an initial pupil performance which is not far from the requested stability. The first pupil stability measure is shown on Figure 10 - left. Pupil stability simulations show that this kind of error is linked to an M3 misalignment. After correction of this alignment, and final optimization of the pupil stability with M2 hexapod, the final performance is given in Figure 10 – right. The achieved stability is well within specification.

Figure 9. Installation of the pupil imaging camera onto the Nasmyth table

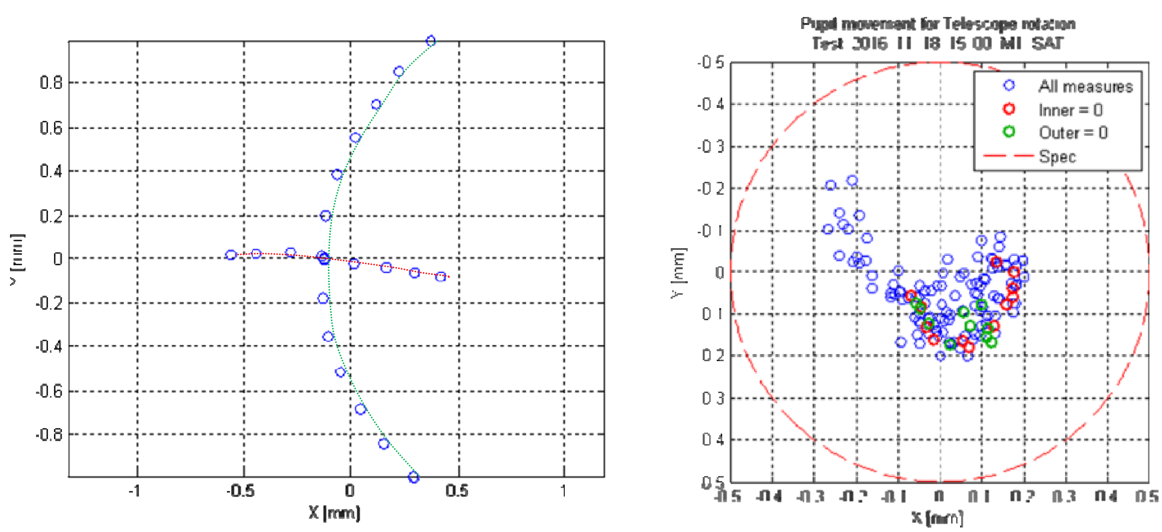

Figure 10. Pupil stability measures. Left: first measure – Right: final measure after fine alignment.

5.3 Telescope final alignment

The pupil being aligned, the telescope is ready to track stars. The next step is thus to elaborate a first pointing model to allow smooth operation of the telescope. Then the image quality is measured thanks to the wave front sensor (WFS) installed close to the Nasmyth table, and the telescope fine alignment is done based on the image quality measurements.

The telescope being installed in the VCMF building, the accessible field of regard (FOR) is reduced with respect to the final dome:

- Star elevation goes from ~30 deg to ~60 deg
- Star azimuth ranges from ~70 deg West from North to ~20 deg East from North

First measurement of image quality with the WFS indicate mainly residual Coma of around 250nm RMS. This was corrected by adjusting M1 rotation. This alignment does not impact the pupil position and the pupil stability performance is thus maintained.

After this first alignment, the image quality was tested in the accessible FOR and at different tube temperatures (depending on the environmental conditions). A typical measurement provided by the WFS is given in Figure 11. The residual error is dominated by astigmatism. Focus and coma are almost eliminated by the hexapod correction. The wavefront error (WFE) measurement in the FOR allows to fit preliminary laws to compensate the focus and coma due to gravity and thermal deformations of the tube. The focus and coma are corrected by moving M2 hexapod (with a combination of decenter and tilt which does not move the pupil). This calibration ends up with five calibration laws (one for each degree of freedom of M2) depending on the tube temperature and the telescope mount position. The total fitting error of the open loop law (in focus and coma) is 34 nm RMS, which is fully in line with the allocated budget of 37 nm RMS.

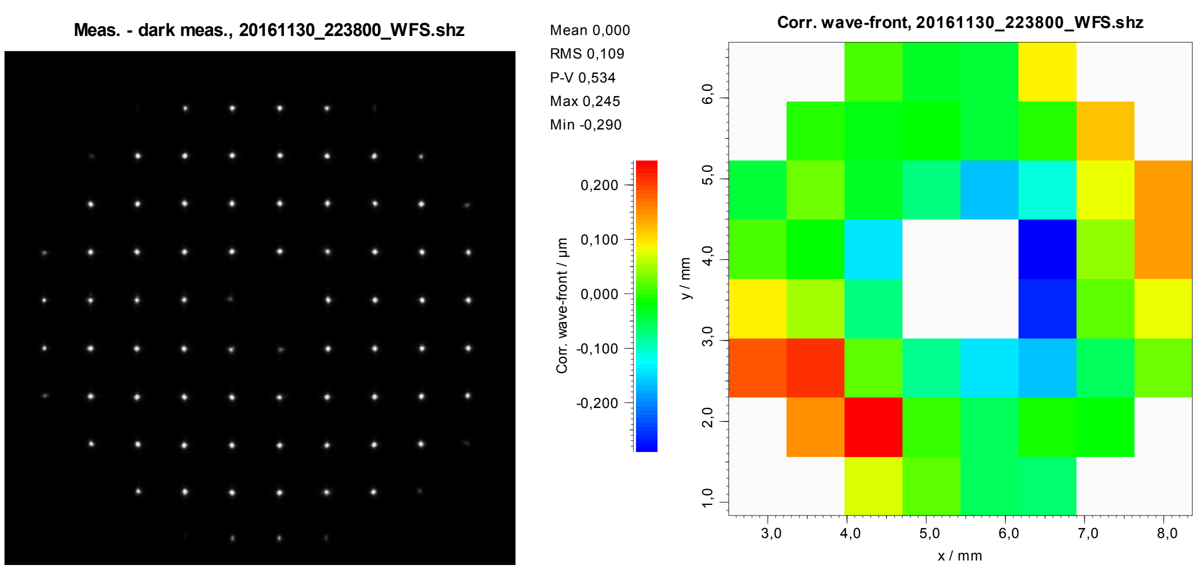

Figure 11. Telescope WFE: WFS spot pattern and WFE map

5.4 Pointing and tracking tests

After final alignment, pointing and tracking performance can be measured.

For the pointing tests, images of ~20 stars spread over the field of regard are recorded (see Figure 12). The telescope uses its pointing model to drive the axes towards the selected stars. The image of the star is recorded on the First Light Camera (FLC). The centroids of these stars are computed. The centroids dispersion in root mean square gives the pointing error. The pointing test result is given in Figure 13. The performance is fully in line with the specification.

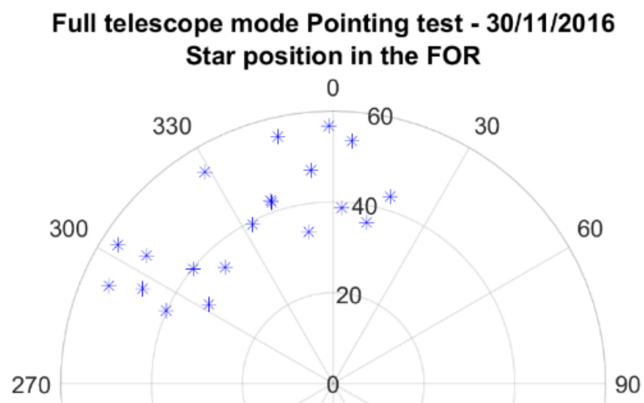

Figure 12. Star positions in the FOR for full telescope pointing and tracking test

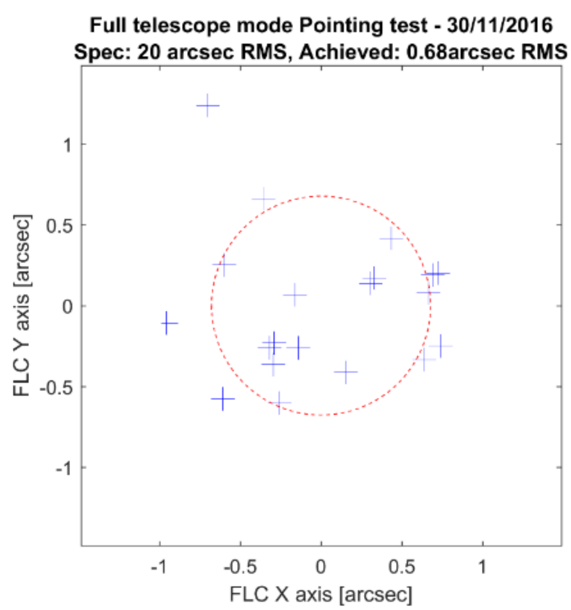

Figure 13. Pointing error measurements

The tracking error is specified on two timescales: 20 and 100 seconds. Centroid acquisitions on each star is thus made on two minutes to allow verifying the requirements. The rms error on intervals of 20 and 100 seconds is then computed, leading to typical measures like Figure 14. The tracking performance verification has been made simultaneously with the pointing test, on the stars shown on Figure 12. In all cases, the performance is better than 0.8 arcsec RMS, although several measures are disturbed by strong seeing. Under normal seeing, the performance improves down to ~0.3 arcsec RMS. This performance is compliant to the specification.

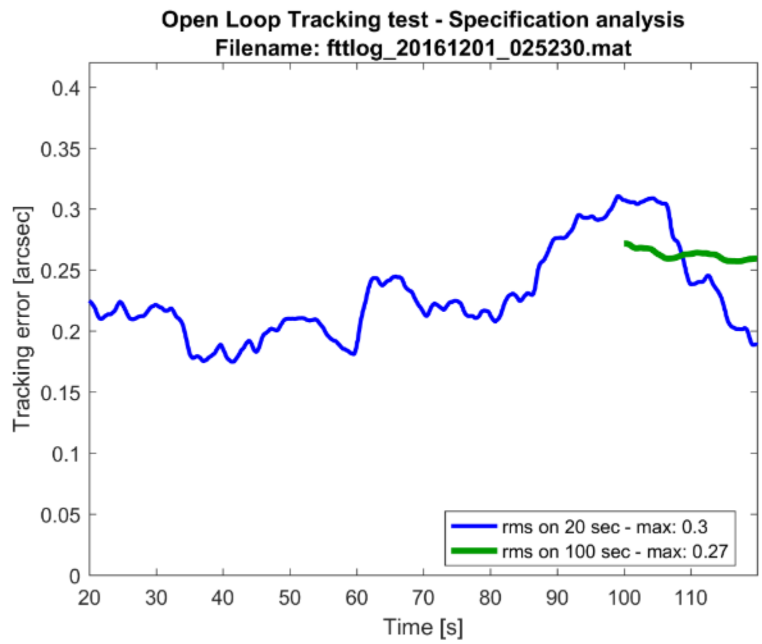

Figure 14. Typical tracking error measurement

The MROi unit telescope can also be used in “tube-offset mode”, were the star image is directly reflected by the flat M3 mirror, while the telescope tube is offset such that the secondary mirror is not blocking the direct view of the starlight. Pointing and tracking requirements shall also be met in this special mode. This has been verified by test, and the performance is in line with the specification.

6. CONCLUSIONS

The integration and alignment of the first of the MROi unit telescope has been successfully performed by AMOS. The position and orientation of the three mirrors of the telescope have been finely adjusted based on pupil and image quality measurements, allowing to achieve the requested performance. The pointing of the telescope has been calibrated and a sub arcsecond pointing accuracy has been measured (on the reduced field of regard). The mount control system has been finely tuned and the tracking performance has been measured on encoder and on sky. The performance is compliant with the specification.

Thanks to the deep testing of the telescope which was made in factory, the verification of the telescope performance on site has been made in a very short timescale (less than one month). This also shows the valuable experience acquired by AMOS for more than 25 years in design, assembly, integration and testing of optical telescopes. As during the design phases of the projects, the strength of AMOS originates from the combination of skills and knowledge in optical, mechanical, thermal, mechatronic and software fields.

The next steps in the frame of the MROi project is the installation of the first unit telescope into its dome, and the completion of the second and third unit telescopes in factory.

REFERENCES

1. Buscher, D. F., Bakker, E. J., Coleman, T. A., et al., "The Magdalena Ridge Observatory Interferometer: a high sensitivity imaging array," Proc. SPIE 6307, - (2006).
2. Pirnay, O., Gloesener, P., Gabriel, E., Graillet, F. and Delrez, Ch., "Design of the unit telescopes of the MROI," Proc. SPIE 7013, - (2008).
3. Mayer, C. J., et al., "The control system for the unit telescopes of the Magdalena Ridge Observatory interferometer," Proc. SPIE 7019, - (2008).
4. Pirnay, O., Pierard, M., Moreau, V., Verheyden, P., & Mayer, C., "Magdalena Ridge Interferometer: assembly, integration and testing of the unit telescopes". Proc SPIE 7734, - (2010)